



Contents lists available at ScienceDirect

## Biochemical Engineering Journal

journal homepage: [www.elsevier.com/locate/bej](http://www.elsevier.com/locate/bej)

Regular article

## Light wavelength distribution effects on the growth rate of *Scenedesmus quadricauda*

Ignacio Niizawa <sup>a,b</sup>, Rodrigo Jorge Leonardi <sup>a,b</sup>, Horacio Antonio Irazoqui <sup>a,b,\*</sup>,  
Josué Miguel Heinrich <sup>a,b,\*</sup>

<sup>a</sup> Group of Innovation on Bio-processes Engineering, Instituto de Desarrollo Tecnológico para la Industria Química (Universidad Nacional del Litoral and Consejo Nacional de Investigaciones Científicas y Técnicas), Ruta Nacional No. 168, 3000 Santa Fe, Argentina

<sup>b</sup> Group of Innovation on Bio-processes Engineering, Facultad de Bioquímica y Ciencias Biológicas, Universidad Nacional del Litoral, Ruta Nacional No. 168 Paraje el Pozo, 3000 Santa Fe, Argentina

### ARTICLE INFO

#### Article history:

Received 20 April 2016

Received in revised form 5 September 2016

Accepted 9 September 2016

Available online xxx

### ABSTRACT

One of the main problems posed by the growth of microalgae is to achieve efficient lighting in the photobioreactors (PBRs). Poor distribution of light within the culture can cause that real productivity achieved in large scale reactors is two to three orders of magnitude lower than those achievable with better distributions. Physical and mathematical modeling is a valuable tool for the design and optimization of these type of bioprocesses. In this study, kinetic models of the growth rate of *Scenedesmus quadricauda* and of the production rate of chlorophylls, were proposed. These models consider the influence of the radiation wavelength composition and of monochromatic light density on microalgal cultures. The parameters of the kinetic model were regressed from experimental data by using a main computer program based on a Genetic Algorithm (GA), supported by a home-built subroutine that consists on a Monte Carlo (MC) simulator for predicting the values of the relevant properties of the radiation field, which was developed in previous work. With the proposed kinetic models, it was possible to achieve the correct simulation of different microalgal cultures carried out in two types of PBRs, illuminated with light of different wavelength composition provided by different light emitting diodes (LEDs) arrangements.

© 2016 Elsevier B.V. All rights reserved.

### 1. Introduction

Microalgae are photosynthetic organisms that have shown great potential for the production of large variety metabolites of commercial interest [1], as well as for the bioremediation liquid and gas effluents [2]. One of the main limitations to the growth of these microorganisms is the difficulty for the efficient supply of light to cultures, causing that the productivity currently achieved in large scale reactors are about two to three orders of magnitude lower than expected [3].

Mathematical modeling is a valuable tool for the design, scaling, simulation and optimization of bioprocesses, besides allowing the prediction of the reactor performance under different growth conditions without the need to carry out actual experiments [4]. Difficulties associated with modeling the growth of microalgae, lie

in the complexities of the interaction between radiation and the metabolism of the cells, as well as in the physical aspects of the radiant energy transfer throughout the reactors. It has been observed that changes in the lighting conditions of the reactors affect the production of biomass [5] and the synthesis of pigments [6].

A realistic model of the radiation field properties in microalgal suspensions should include the simultaneous occurrence of absorption and scattering of radiation at any point in the culture [7]. A differential balance of radiant energy including these phenomena gives rise to the Radiation Energy Transfer Equation (RTE). A physical model of the radiant energy field and its corresponding mathematical problem are correctly posed when the boundary conditions which must be fulfilled by the particular solution of the RTE, are realistic descriptions of the phenomena occurring on the walls of the vessel, and especially of the characteristics of the light source [8–10]. Due to the inherent complexity of the problem, an analytic solution remains elusive, and simplifications of the physical model are needed as far as its reliability is not seriously compromised. Among such simplified models and approximate solution methods, we find those based on the Lambert-Beer law [11], the Two-fluxes approximation [12] and the Discrete Ordinate method [13]. To get round the problems inherent to the resolution of the RTE

\* Corresponding authors at: Group of Innovation on Bio-processes Engineering, Instituto de Desarrollo Tecnológico para la Industria Química (Universidad Nacional del Litoral and Consejo Nacional de Investigaciones Científicas y Técnicas), Ruta Nacional No. 168, 3000 Santa Fe, Argentina. Tel.: +54 342 4575215x172.

E-mail address: [heinrichmiguel@hotmail.com](mailto:heinrichmiguel@hotmail.com) (J.M. Heinrich).

we used an approach based on the MC physical simulation of the field distribution of radiant energy in the PBR [14,10]. This method emulates the radiant field by tracking photons, step by step, along their respective paths through a microalgal suspension. In each of these elementary steps, a probability is assigned to the event that the photon is absorbed (i.e., removed from the radiation field), dispersed (i.e. deflected from its previous direction of movement) or lost through the reactor walls. Therefore, an important advantage of the MC method is that predicts the local value of properties of radiant field in a culture of microalgae, considering the characteristics of the light emitted by the light source and those of the suspension of microalgae, making unnecessary the introduction of simplifications in order to obtain approximate solutions of the problem including the RTE and its boundary conditions.

Several authors have led studies to evaluate the efficiency of different intensities as well as of different wavelength compositions of visible light on the growth of cultures of microalgae, using LEDs as radiation source [15–20]. Studies have shown that blue radiation is capable to stimulate lipids accumulation and growth rate of *Chlorella vulgaris* [21]; promote accumulation of β-carotene in *Dunaliella salina* [22] and augment the accumulation of chlorophylls in *Chlamydomonas reinhardtii* [23]. Furthermore, it has been reported that the use of red radiation allows higher biomass production by increasing the tolerance to high radiation intensities in cultures of *Dunaliella salina* [22]; augment accumulation of phycocyanin in cyanobacteria [24] and achieve greater efficiency in the utilization of light for cell growth compared to daylight radiation profiles in cultures of *Haematococcus pluvialis* [25]. Several conclusions on radiation conditions affecting microalgal growth, metabolite synthesis, photosynthesis and morphogenesis have been reported in the literature. Different microalgal species respond differently to light conditions possibly due to the presence and the activity of different kinds of photoreceptors [26]. These photoreceptors sense different light wavelengths and trigger specific protein structural changes through various mechanisms [27].

In this paper a biomass growth kinetics model for a strain of *Scenedesmus quadricauda* is proposed and experimentally validated. Growth conditions were such that the local volumetric rate of photon absorption was the limiting factor of growth and of chlorophyll production. A series of cultures were carried out in PBRs irradiated with light of different wavelength composition using arrays made of blue, green, yellow and red LEDs, which are an emerging and economical technology compared to ordinary fluorescent lamps in microalgae growth because of its lower power consumption, longer life time, lower heat dissipation, smaller mass and volume, single wavelength, and high efficiency of electricity conversion [28].

First, the effect of radiation from each kind of LED on the growth of microalgae has been assessed in separate experiments. Then, a series of cultures were irradiated with light of different wavelength composition, supplied by arrangements of LEDs. The

experimental results obtained, together with the implementation of radiant energy field simulation model, previously developed by our research group [10], were used to develop a computer program based on the GA, for setting the parameters of the proposed growth model. It is expected that the developed kinetic model can be used as a tool for the design and simulation of different types of PBRs.

## 2. Materials and methods

### 2.1. Strain and culture maintenance

The freshwater species *Scenedesmus quadricauda* 276/21 (obtained from CCAP) was grown in 250 ml of BBM culture media adjusted to pH 7, frequently used for the cultivation of freshwater microalgae, in 500 ml Erlenmeyer flasks. The media contain the following components: NaNO<sub>3</sub> (2.94 mM); NaCl (0.428 mM), K<sub>2</sub>HPO<sub>4</sub> (0.431 mM); KH<sub>2</sub>PO<sub>4</sub> (1.29 mM); MgSO<sub>4</sub>·7H<sub>2</sub>O (0.304 mM); CaCl<sub>2</sub>·2H<sub>2</sub>O (0.17 mM); EDTA (0.171 mM); KOH (0.553 mM); H<sub>3</sub>BO<sub>3</sub> (0.185 mM); MnCl<sub>2</sub>·4H<sub>2</sub>O (7.28 10<sup>-3</sup> mM); ZnSO<sub>4</sub>·7H<sub>2</sub>O (3.07 10<sup>-2</sup> mM); MoO<sub>3</sub> (4.93 10<sup>-3</sup> mM); CuSO<sub>4</sub>·5H<sub>2</sub>O (6.29 10<sup>-3</sup> mM); Co(NO<sub>3</sub>)<sub>2</sub>·6H<sub>2</sub>O (1.68 10<sup>-3</sup>); FeSO<sub>4</sub>·7H<sub>2</sub>O (1.79 10<sup>-2</sup> mM) [29]. The cultures were continuously irradiated under 70 μmol photons m<sup>-2</sup> s<sup>-1</sup> using fluorescent lamps at ambient temperature (between 25 and 30 °C) over two weeks prior the experiments.

### 2.2. Microalgal cultures

During the course of this study, two different types of reactors were used. The first experimental apparatus consists in a cylindrical PBR of 2 liters maximum capacity and 137 mm diameter, made of borosilicate glass (Fig. 1a). An air diffuser, consisting of a circular slab of sintered glass was placed at the center on the PBR's bottom.

The other reactor is a commercial bio-fermenter Infors of 3 liters of maximum capacity and 140 mm diameter (Fig. 1b). An air diffuser of stainless steel is placed at the center on the PBR's bottom. Both PBRs in the present paper used the same culture (BBM).

In both cases, the air flow rate was set at 0.4 vvm, in order to provide enough gas-liquid transfer area per unit volume as needed to supply the medium with CO<sub>2</sub>, to remove the O<sub>2</sub> produced by oxygenic photosynthesis and to ensure the correct agitation of the culture.

Cultures were irradiated with various lighting schemes using different arrangements of strips of commercial LEDs. The wavelength emission range of the different type of LEDs are: 420–490 nm the Blue LED, 480–560 nm the Green LED, 550–640 nm the yellow and 610–670 nm the Red LED. The range of wavelength emission and the rate of photon emission of each type of LED were determined with an OCEAN OPTICS spectrophotometer (Table 1).

In order to study the influence of light wavelength on the production of biomass and chlorophylls, four essays were independently realized in the PBR of 2L (Fig. 1a) illuminated with

**Table 1**

Type of LEDs and number of units in each array, with indication of the corresponding total rate of emission of photons and the total photon flux density on the external wall of the PBR.

| Reactor           | Culture       | Number and type of LEDs | Rate of emission of photons (μmol photons sec <sup>-1</sup> LED <sup>-1</sup> ) | Total photon flux density (μmol photons/L <sup>-1</sup> sec <sup>-1</sup> ) |
|-------------------|---------------|-------------------------|---|---|
| 2L Reactor        | Blue          | 24 blue LEDs            | 10.58 10 <sup>-2</sup>  | 1.27  |
|                   |               | 48 green LEDs           | 6.13 10 <sup>-2</sup>   | 1.47  |
|                   |               | 216 yellow LEDs         | 1.12 10 <sup>-2</sup>   | 1.21  |
|                   |               | 48 red LEDs             | 5.18 10 <sup>-2</sup>   | 1.24  |
| 3L INFORS Reactor | Full Spectrum | 30 blue LEDs            | 10.58 10 <sup>-2</sup>  | 1.06  |
|                   |               | 60 red LEDs             | 5.18 10 <sup>-2</sup>   | 1.04  |
|                   |               | 54 green LEDs           | 6.13 10 <sup>-2</sup>   | 1.10  |
|                   |               | 288 yellow LEDs         | 1.12 10 <sup>-2</sup>   | 1.13  |

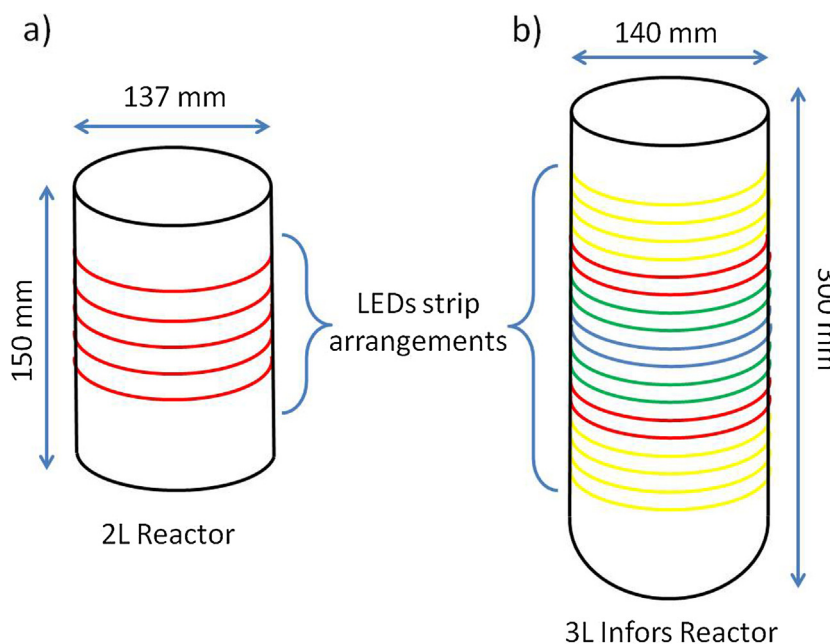


**Fig. 1.** (a) Diagram of the 2 liters borosilicate glass PBR with a LEDs strip arrangement fastened on the external wall; (b) Diagram of the 3 liters Infors reactor used in full spectrum cultures with a LEDs strip arrangement fastened on the external wall.

arrangements made of blue, green, yellow and red LEDs in different numbers, keeping in all cases about the same total number of photons received by the PBR per unit of time (Table 1).

Moreover, a culture was carried out in the reactor INFORS (full spectrum culture) using a radiation source that combines the four types of LEDs used above (Fig. 1b). The number of LEDs used in this case allows the PBR receiving higher radiation intensity, with a similar number of photons per unit time and volume than the blue, green, yellow and red cultures combined.

In all cases 50 ml samples were taken daily during the time of cultivation (10–14 days). Simultaneously, the culture was replenished with the same volume of fresh medium.

The reactor was isolated from external radiation, and its temperature was controlled between 25–28 °C during each experimental run. Three different cultures were performed independently for each lighting condition. All three cultures yielded similar results in terms of the concentration of biomass and chlorophylls content.

### 2.3. Biomass analysis

The algal biomass concentration was followed during growth by measuring the amount of total suspended solids; 30 ml of the sample were centrifuged at 5000 rpm over 10 min. Then the pellet was once washed with distilled water and was dried at 80 °C overnight.

### 2.4. Chlorophylls analysis

The concentrations of chlorophylls a and b in microalgae suspensions, were determined using the photo-colorimetric technique proposed by Ritchie [30], using 100% ethanol for extraction. Chlorophylls concentrations were correlated with optical densities as follows:

$$\text{Chlorophyll } a (\text{mg/L})$$

$$= (-5.2007 \text{ OD}_{649 \text{ nm}} + 13.5275 \text{ OD}_{665 \text{ nm}}) / \text{optical path} \quad (1)$$

$$\text{Chlorophyll } b (\text{mg/L})$$

$$= (22.4327 \text{ OD}_{649 \text{ nm}} - 7.0741 \text{ OD}_{665 \text{ nm}}) / \text{optical path} \quad (2)$$

### 2.5. Modeling of cell growth in cultures of microalgae irradiated with light of different spectral composition

The physical and mathematical model of radiant energy field in cultures of microalgae conducted in PBPs, as well as the supporting algorithm used for its computational implementation were developed in previous work [10]. In that model, it is considered that the spectral distribution of the local rate of absorption of photons  $r_{\lambda}^{\text{abs}}(r, t) [\mu\text{mol photons day}^{-1} L^{-1}]$  at any position  $r$  at the instant  $t$ , is the property linking the radiant energy field and the production rate of biomass and chlorophylls in microalgae. In particular, the unstructured kinetic expression proposed by Aiba [31] to represent the local rate of growth of microorganisms, is chosen in this work for the particular case of *Scenedesmus quadricauda*

$$r_{x,\text{PAR}}(r, t) = \sum_{\lambda} r_{x,\lambda}(r, t) \quad (3)$$

where  $r_{x,\text{PAR}}(r, t) [\text{mg biomass L}^{-1} \text{ day}^{-1}]$  is the local biomass production rate corresponding to the photosynthetically active radiation (PAR) at each point of the reactor  $r$  at the instant  $t$ , and

$r_{x,\lambda}(r, t) [\text{mg biomass L}^{-1} \text{ day}^{-1}]$  is the local biomass production rate corresponding to the spectral regions of emission of the different LEDs used (i.e., blue, green, yellow and red) at each point of the reactor  $r$  at the instant  $t$ , defined as:

$$r_{x,\lambda}(r, t) = \frac{\mu_{\lambda}^x r_{\lambda}^{\text{abs}}(r, t)}{x(t) + K_{1,\lambda}^x r_{\lambda}^{\text{abs}}(r, t) K_{2,\lambda}^x r_{\lambda}^{\text{abs}}(r, t)^2} x(t) \quad (4)$$

In Eq. (4)  $x(t) [\text{mg L}^{-1}]$  is the concentration of microalgae at the instant  $t$ ,  $\mu_{\lambda}^x$ ,  $K_{1,\lambda}^x$  and  $K_{2,\lambda}^x$  are kinetic constants corresponding to the spectral regions of emission of the different LEDs and  $r_{\lambda}^{\text{abs}}(r, t) [\mu\text{mol photons L}^{-1} \text{ day}^{-1}]$  is the local rate of absorption of photons corresponding to the spectral regions of emission of the different LEDs at any position  $r$  at the instant  $t$ . It can be seen that the model allows for saturation and cell growth inhibition depending on the culture irradiation conditions [32].

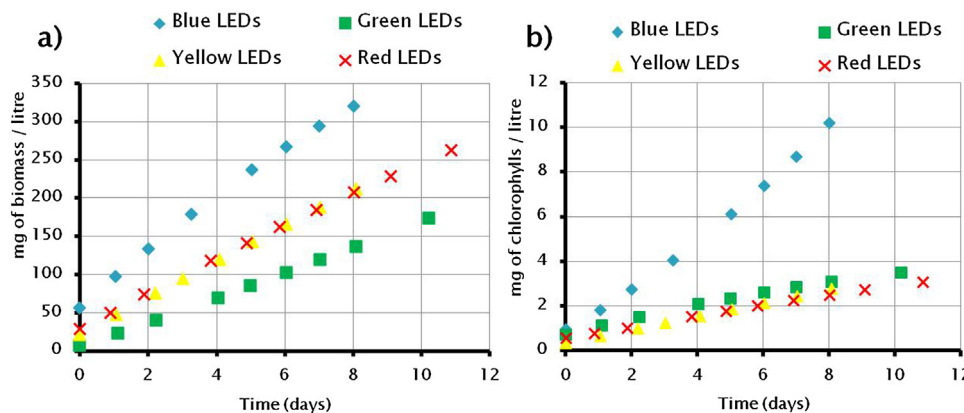


**Fig. 2.** Time evolution of the concentration of biomass (a) and of total chlorophylls (b) in cultures of *Scenedesmus quadricauda* illuminated with arrangements of LEDs of the same color: red, yellow, green or blue.

The local rate of chlorophylls production,  $r_{chl,PAR}(r, t)$  [chlorophyll mg L<sup>-1</sup> day<sup>-1</sup>], corresponding to the PAR at each point of the reactor  $r$  at the instant  $t$ , is assumed to be the result of adding the individual monochromatic rates

$$r_{chl,PAR}(r, t) = \sum_{\lambda} r_{chl,\lambda}(r, t) \quad (5)$$

Furthermore, the monochromatic rates of production of chlorophylls were modeled as functions which increase with the corresponding monochromatic local rate of photon absorption, progressively showing saturation for larger values of the rate of photon absorption

$$r_{chl,\lambda}(r, t) = \frac{\mu_{\lambda}^{chl} r_{\lambda}^{abs}(r, t)}{c_{chl}(t) + K_{1,\lambda}^{chl} r_{\lambda}^{abs}(r, t)} x(t) \quad (6)$$

In Eq. (6)  $\mu_{\lambda}^{chl}$  and  $\mu_{\lambda}^{chl}$  are constants corresponding to the spectral regions of emission of the different LEDs used;  $r_{\lambda}^{abs}(r, t)$  [ $\mu\text{mol photons day}^{-1}\text{L}^{-1}$ ] is the local rate of absorption of photons at each point in the reactor at the instant  $x(t)$  [mg L<sup>-1</sup>] is the concentration of microalgae at the instant  $c_{chl}$  [mg L<sup>-1</sup>] is the total concentration of chlorophylls in the microalgal suspension at the instant  $t$ , and  $r_{chl,\lambda}(r, t)$  [chlorophyll mg L<sup>-1</sup> day<sup>-1</sup>], is the local rate of chlorophylls production corresponding to each of the spectral regions of emission of the different LEDs used, at each point in the reactor at the instant  $t$ .

It was observed that photons belonging to different regions of the visible spectrum used in this work show different efficiencies for the chlorophylls production.

The parameters of the kinetic model which is shown in Eq. (4) and Eq. (6) were regressed from experimental data by using a main computer program based on a GA [33], supported by a home-built subroutine that consists on a MC simulator for predicting the values of the relevant properties of the radiation field [10].

For the validation of the proposed model, predicted values of the production of biomass and chlorophyll will be compared with

experimental data obtained from cultures grown under radiation of different wavelength compositions.

### 3. Results and discussion

#### 3.1. Microalgal cultures under different radiation composition

Fig. 2 shows the time evolution of the concentration of biomass (a) and that of total chlorophylls (b) in the cultures irradiated with one of the four types of LEDs each time.

The concentrations of biomass and of total chlorophylls, in all cases increase with time in a practically linear way throughout the period of study. The average rate of biomass and chlorophylls production under different lighting conditions are shown in Table 2.

The average rate of biomass production ( $\Delta x/\Delta t$ ) in the Blue culture was greater than in the others. Cultures receiving yellow and red radiation showed growth profiles similar to each other. The emission profile of green LEDs largely coincides with the “green window” of the visible radiation spectrum [34], explaining the lowest  $\Delta x/\Delta t$  value observed in culture 2.

Moreover, the values of the average rate of chlorophylls production ( $\Delta c_{ch}/\Delta t$ ) achieved in the green, yellow and red cultures are very similar to each other; while in the PBR irradiated with blue LEDs a greater value of  $\Delta c_{ch}/\Delta t$  is attained.

Analyzing the production values of chlorophylls per unit biomass ( $\Delta c_{ch}/\Delta x$ ), it is noted that of Blue culture is markedly greater than the others; although the Green culture achieves a  $\Delta c_{ch}/\Delta x$  value greater than those in the Yellow and Red culture.

Full spectrum culture was irradiated with the 4 types of LEDs, and received almost four times the radiation flux density of each previous cultures (Table 1). The biomass and total chlorophylls concentrations attained are far greater than those of the previous cases (Fig. 3).

According to results shown in Table 2, the average rate of biomass production in Full Spectrum culture is proportional to the

**Table 2**  
Average rate of biomass and chlorophylls production under the different lighting conditions.

| Reactor           | Culture       | $\Delta x/\Delta t$ [mg of biomass/L <sup>-1</sup> day <sup>-1</sup> ] | $\Delta c_{ch}/\Delta t$ [mg of chlorophyll/L <sup>-1</sup> day <sup>-1</sup> ] | $\Delta c_{ch}/\Delta x$ [mg of chlorophyll/mg of biomass <sup>-1</sup> ] |
|-------------------|---------------|--|---|---|
| 2L Reactor        | Blue          | 34.38  | 1.09  | $3.17 \cdot 10^{-2}$  |
|                   | Green         | 15.98  | 0.29  | $1.81 \cdot 10^{-2}$  |
|                   | Yellow        | 23.79  | 0.30  | $1.26 \cdot 10^{-2}$  |
|                   | Red           | 21.51  | 0.23  | $1.07 \cdot 10^{-2}$  |
| 3L Infors Reactor | Full Spectrum | 94.82  | 2.70  | $2.85 \cdot 10^{-2}$  |

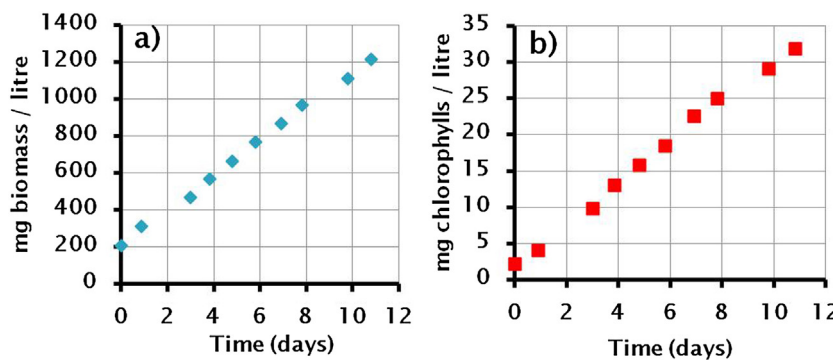


**Fig. 3.** Evolution over time of biomass (a) and total chlorophylls (b) concentrations in *Scenedesmus quadricauda* cultures combining the four types of LEDs.

growth rates observed in previous cultures. Furthermore, the value of  $\Delta c_{ch}/\Delta x$  reached, is very similar to that of blue culture.

The use of different radiation profiles for microalgae cultivation generates changes on cell growth. Blue radiation promotes the increase of chlorophylls concentration in microalgae cells, which are reordered so that to increase their presence in the light-harvesting complex and reaction centers augmenting the size of the photo-system II (PSII) [35]. The adaptation of microalgae to the prevailing light condition implies the action of photoreceptors which modulate these effects. Microalgae have different photoreceptors acting on the blue visible radiation spectrum region (cryptochromes). It is reported that the genus *Scenedesmus* has this type of photoreceptor and that they act by stimulating the synthesis of chlorophylls according to the radiation intensity and profile received [26].

Photoreceptors have evolved to increase the quantum yield for producing a signal and to minimize the non-productive deactivation process. This means that the activation of the chromophore must be efficient, specific, and very fast [36]. Thus even when a small fraction of green LED emission profile correspond to the blue region of the visible spectrum or when different LEDs are combined with the blue LEDs (full spectrum culture), the absorption of these photons would be sufficient to achieve activation of the photoreceptor and induce greater accumulation of chlorophylls.

The differences observed in the microalgae culture development under different lighting profiles, exhibit the importance of analyzing the effect of the different radiation spectrum regions on microalgal growth.

### 3.2. Microalgae growth modeling in PBRs illuminated with light comprising various wavelengths

The parameters of the kinetic model which is shown in Eq. (4) and Eq. (6) were regressed from experimental data by using a main computer program based on a GA, supported by a home-built subroutine that consists on a MC simulator for predicting the values of the relevant properties of the radiation field, which correspond to the current values of the parameters. The “best” set of parameters is that which minimizes the target function  $\sqrt{(x_{exp}(t) - x_{prog}(t))^2}$  (where  $x_{exp}(t)$  is the experimental biomass concentration at the instant  $t$  and  $x_{prog}(t)$  is the predicted biomass concentration at the instant  $t$ , by the program developed), which measures the discrepancy between experimental and predicted values of the time-dependent concentration of biomass and that of chlorophylls. The “best” set of constants found is reported in Table 3.

Simulated and experimental results of biomass and chlorophylls production under different conditions of illumination are shown in Figs. 4–6.

In Table 4 are shown the corresponding  $R^2$  values for the correlations between the experimental and the simulated values of biomass and chlorophyll concentration on each culture.

It can be observed a good agreement between model predictions and experimental data, both in cultures using a single type of LED as in that combining all of them, thus showing the wide range of situations covered by the growth kinetic model proposed.

**Table 3**

Kinetic model for biomass and chlorophyll production of *Scenedesmus quadricauda*: best fit parameters.

Growth kinetic model for *Scenedesmus quadricauda*: best fit parameters

|  |                |  |                |
|--|----------------|--|----------------|
| $\mu_{Blue}^x$ $\left[ \frac{\text{biomass mg}}{\mu\text{mol photons}} \right]$                        | 9.88 $10^{-4}$ | $K_{1, Yellow}^x$ $\left[ \frac{\text{biomass mg day}}{\mu\text{mol photons}} \right]$               | 6.61 $10^{-6}$ |
| $\mu_{Green}^x$ $\left[ \frac{\text{biomass mg}}{\mu\text{mol photons}} \right]$                       | 1.56 $10^{-3}$ | $K_{1, Red}^x$ $\left[ \frac{\text{biomass mg day}}{\mu\text{mol photons}} \right]$                  | 4.19 $10^{-5}$ |
| $\mu_{Yellow}^x$ $\left[ \frac{\text{biomass mg}}{\mu\text{mol photons}} \right]$                      | 1.49 $10^{-3}$ | $K_{2, Blue}^x$ $\left[ \frac{\text{biomass mg}^2 \text{ day}^2}{\mu\text{mol photons}^2} \right]$   | 4.23 $10^{-8}$ |
| $\mu_{Red}^x$ $\left[ \frac{\text{biomass mg}}{\mu\text{mol photons}} \right]$                         | 6.33 $10^{-4}$ | $K_{2, Green}^x$ $\left[ \frac{\text{biomass mg}^2 \text{ day}^2}{\mu\text{mol photons}^2} \right]$  | 1.67 $10^{-7}$ |
| $K_{1, Blue}^x$ $\left[ \frac{\text{biomass mg day}}{\mu\text{mol photons}} \right]$                   | 6.72 $10^{-6}$ | $K_{2, Yellow}^x$ $\left[ \frac{\text{biomass mg}^2 \text{ day}^2}{\mu\text{mol photons}^2} \right]$ | 8.06 $10^{-8}$ |
| $K_{1, Green}^x$ $\left[ \frac{\text{biomass mg day}}{\mu\text{mol photons}} \right]$                  | 2.10 $10^{-4}$ | $K_{2, Red}^x$ $\left[ \frac{\text{biomass mg}^2 \text{ day}^2}{\mu\text{mol photons}^2} \right]$    | 4.24 $10^{-8}$ |
| $\mu_{Blue}^{chl}$ $\left[ \frac{\text{chlorophyll mg}^2}{\mu\text{mol photons biomass mg}} \right]$   | 4.13 $10^{-7}$ | $K_{Blue}^{chl}$ $\left[ \frac{\text{chlorophyll mg day}}{\mu\text{mol photons}} \right]$            | 1.02 $10^{-5}$ |
| $\mu_{Green}^{chl}$ $\left[ \frac{\text{chlorophyll mg}^2}{\mu\text{mol photons biomass mg}} \right]$  | 2.20 $10^{-6}$ | $K_{Green}^{chl}$ $\left[ \frac{\text{chlorophyll mg day}}{\mu\text{mol photons}} \right]$           | 7.42 $10^{-4}$ |
| $\mu_{Yellow}^{chl}$ $\left[ \frac{\text{chlorophyll mg}^2}{\mu\text{mol photons biomass mg}} \right]$ | 2.76 $10^{-6}$ | $K_{Yellow}^{chl}$ $\left[ \frac{\text{chlorophyll mg day}}{\mu\text{mol photons}} \right]$          | 1.19 $10^{-4}$ |
| $\mu_{Red}^{chl}$ $\left[ \frac{\text{chlorophyll mg}^2}{\mu\text{mol photons biomass mg}} \right]$    | 8.76 $10^{-8}$ | $K_{Red}^{chl}$ $\left[ \frac{\text{chlorophyll mg day}}{\mu\text{mol photons}} \right]$             | 1.57 $10^{-5}$ |

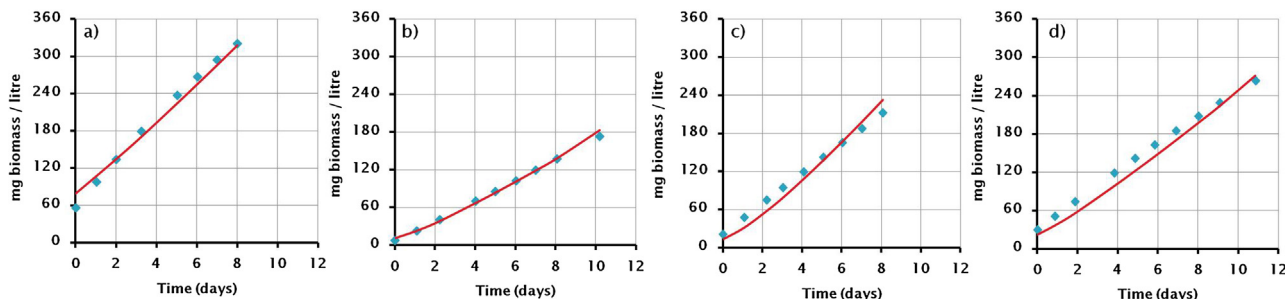


**Fig. 4.** Validation of the kinetic model for biomass production. Concentration over time in cultures of *Scenedesmus quadricauda* lighted with arrangements of LEDs of same color: (a) blue LEDs; (b) green LEDs; (c) yellow LEDs; (d) red LEDs. The blue diamond represents experimental data while red lines represent the corresponding predicted values.

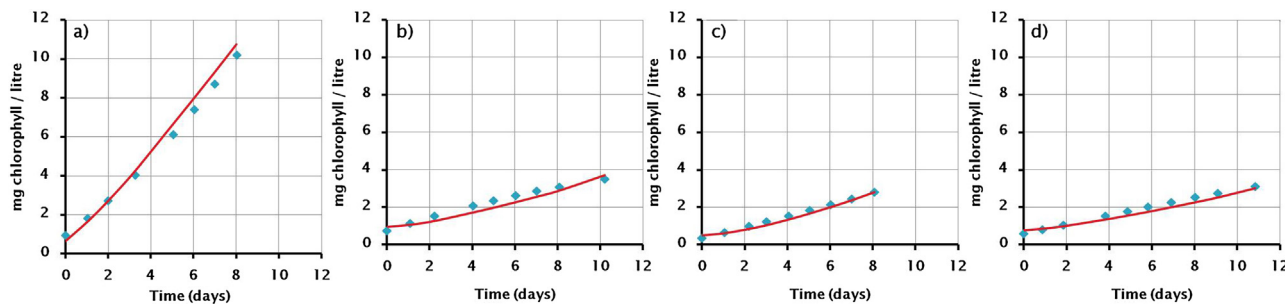


**Fig. 5.** Validation of the kinetic model for chlorophylls production. Chlorophylls concentration over time in cultures of *Scenedesmus quadricauda* lighted with arrangements of LEDs of same color: (a) blue LEDs; (b) green LEDs; (c) yellow LEDs; (d) red LEDs. The blue diamond represents experimental data while red lines represent the corresponding predicted values.

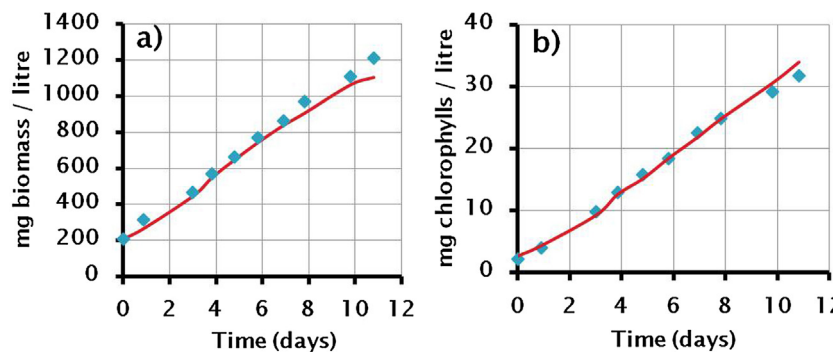


**Fig. 6.** Validation of the kinetic models for biomass and chlorophylls production in *Scenedesmus quadricauda* cultures lighted by a combination of the four types of LEDs: Evolution over time of biomass (a) and total chlorophylls (b) concentrations. The blue diamond represents experimental data while red lines represent the corresponding predicted values.

**Table 4**

Corresponding  $R^2$  values for the correlation between the experimental and the simulated values of biomass and chlorophyll production on each culture.

| Reactor           | Culture       | $R^2$ for biomass production | $R^2$ for chlorophyll production |
|-------------------|---------------|------------------------------|----------------------------------|
| 2L Reactor        | Blue          | 0.994                        | 0.995                            |
|                   | Green         | 0.975                        | 0.898                            |
|                   | Yellow        | 0.929                        | 0.954                            |
|                   | Red           | 0.948                        | 0.962                            |
| 3L Infors Reactor | Full Spectrum | 0.993                        | 0.992                            |

### 3.3. Analysis of the spatial distribution of the local rate of photon absorption and of the local biomass production rate in the full spectrum culture

The monochromatic local rate of absorption of photons,  $r_{\lambda}^{abs}(r, t)$ , was predicted at every point in the culture using the simulation program based on a Monte Carlo algorithm previously developed [10]. These results together with the set of “best fit” kinetic parameters obtained as described earlier in this work

enabled us to predict the monochromatic local rate of growth of biomass (Eq. (4)), as well as the monochromatic local rate of chlorophylls production  $r_{chl,\lambda}(r, t)$  (Eq. (6)). This was done for different configurations of the light source, and in the figures that follow, are shown as contour curves for different biomass concentrations which are attained by the culture as it evolves in time.

In the contour graphs of Fig. 7 the local values of  $r_{PAR}^{abs}(r, t)$  and  $r_{x,PAR}(r, t)$  are shown for different biomass concentrations reached by the full spectrum culture during its evolution in time.

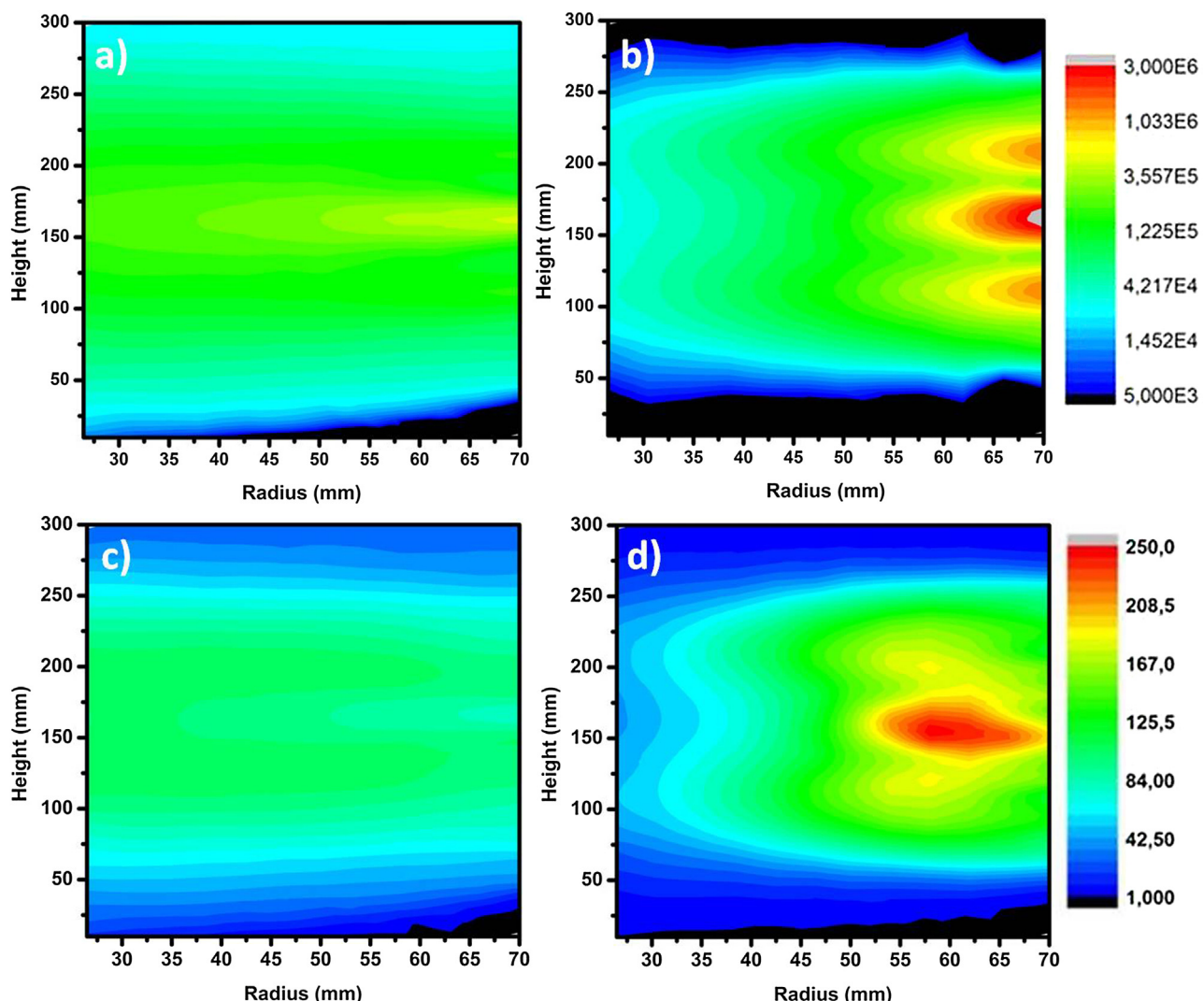


**Fig. 7.** Distribution profiles of  $r_{PAR}^{abs}(r, t)$  [ $\mu\text{mol photons day}^{-1}\text{L}^{-1}$ ] and  $r_{x,PAR}(r, t)$  [ $\text{mg biomass L}^{-1}\text{ day}^{-1}$ ] in the 3L Infors reactor at different stages of Full spectrum culture. (a)  $r_{PAR}^{abs}(r, t)$  (200 mg biomass/L); (b)  $r_{PAR}^{abs}(r, t)$  (1200 mg biomass/L); (d)  $r_{x,PAR}(r, t)$  (200 mg biomass/L); (e)  $r_{x,PAR}(r, t)$  (1200 mg biomass/L).

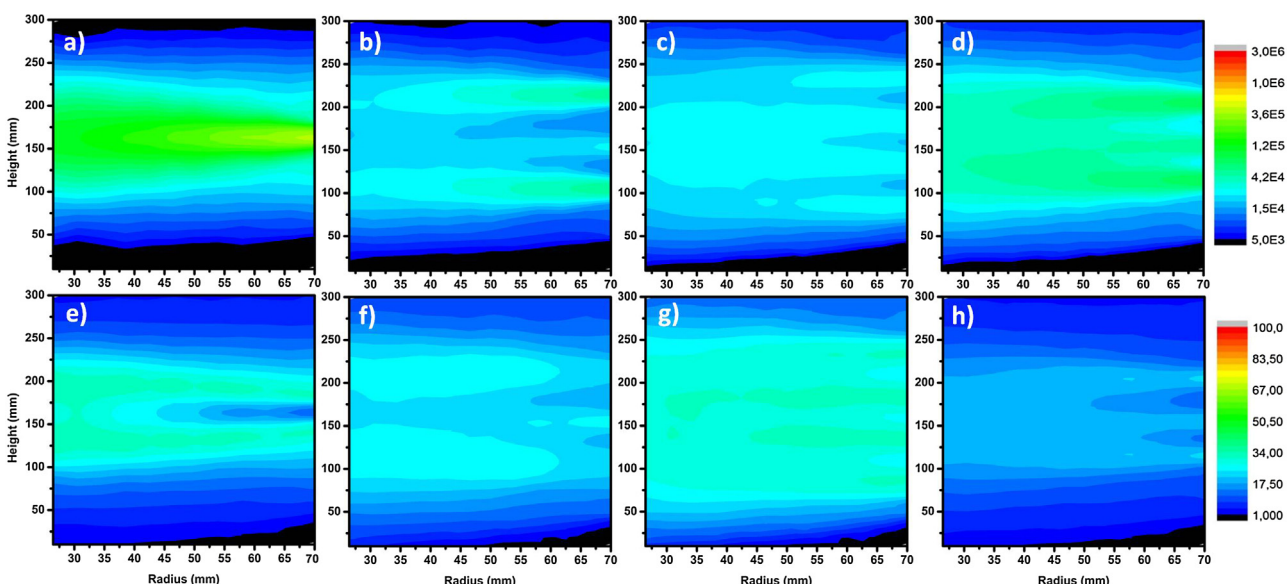


**Fig. 8.** Distribution profiles of  $r_{\lambda}^{abs}(r, t)$  [ $\mu\text{mol photons day}^{-1}\text{L}^{-1}$ ] and  $r_{x,\lambda}(r, t)$  [ $\text{mg biomass L}^{-1}\text{ day}^{-1}$ ] in full spectrum culture inside the 3L Infors reactor at 200 mg biomass/L. (a)  $r_{Blue}^{abs}(r, t)$ ; (b)  $r_{Green}^{abs}(r, t)$ ; (c)  $r_{Yellow}^{abs}(r, t)$ ; (d)  $r_{Red}^{abs}(r, t)$ ; (e)  $r_{x,Blue}(r, t)$ ; (f)  $r_{x,Green}(r, t)$ ; (g)  $r_{x,Yellow}(r, t)$ ; (h)  $r_{x,Red}(r, t)$ .

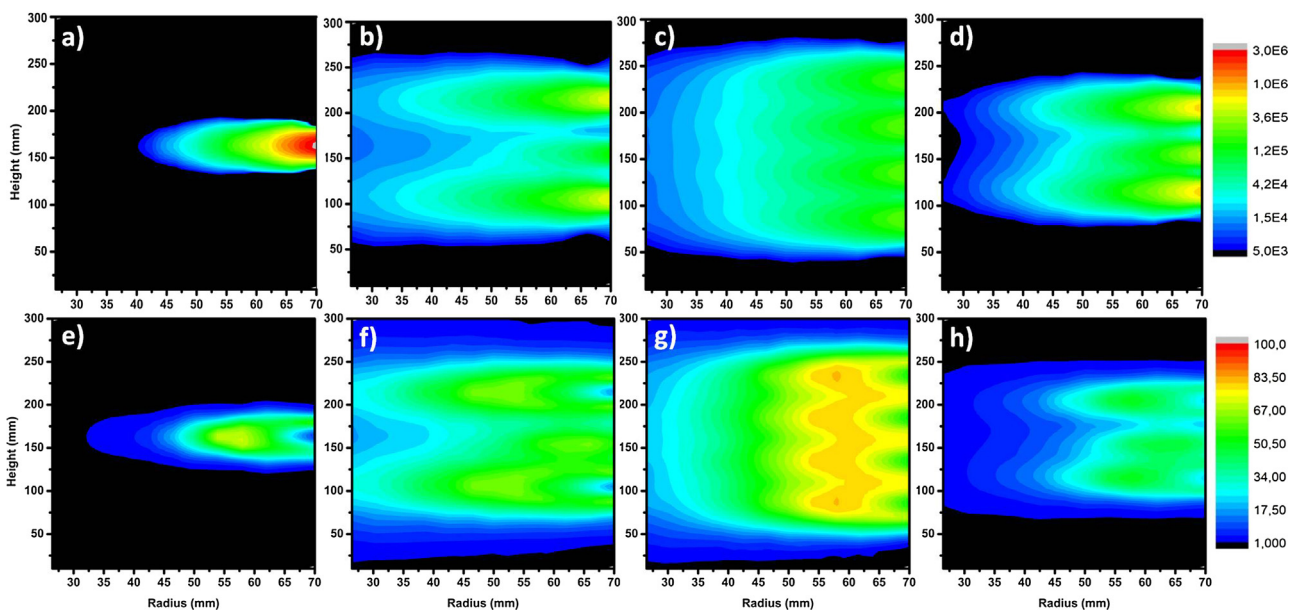


**Fig. 9.** Distribution profiles of  $r_{\lambda}^{abs}(r, t)$  [ $\mu\text{mol photons day}^{-1}\text{L}^{-1}$ ] and  $r_{x,\lambda}(r, t)$  [ $\text{mg biomass L}^{-1}\text{day}^{-1}$ ] in full spectrum culture inside the 3L Infors reactor at 1200 mg biomass/L. (a)  $r_{Blue}^{Abs}(r, t)$ ; (b)  $r_{Green}^{Abs}(r, t)$ ; (c)  $r_{Yellow}^{Abs}(r, t)$ ; (d)  $r_{Red}^{Abs}(r, t)$ ; (e)  $r_{x,Blue}(r, t)$ ; (f)  $r_{x,Green}(r, t)$ ; (g)  $r_{x,Yellow}(r, t)$ ; (h)  $r_{x,Red}(r, t)$ .

In order to analyze the individual effect of different visible radiation spectrum regions on microalgal growth; in Figs. 8 and 9 are displayed the distribution of  $r_{\lambda}^{abs}(r, t)$  and  $r_{x,\lambda}(r, t)$  in the 3L Infors reactor (Fig. 1b) at two different stages of the culture, independently analyzing the effect of radiation profile of each type of LED.

Figs. 8 and 9(a)–(d), show that the rate of photon absorption in cultures lighted with blue or red LEDs is more stratified than in cultures illuminated by green and yellow LEDs. Thus, in the two former cases, the regions closer to the reactor core become darker with increasing concentrations of biomass and chlorophylls, more rapidly than in the latter two situations. As the biomass grows, the more distant regions of the LEDs location will be exposed to a radiation profile enriched in those photons with lower absorption probability (i.e., green and yellow photons).

Figs. 8 and 9(e)–(h) show the effect of the spatial distribution of the rate of photon absorption on the rate of biomass production for different regions of the visible radiation spectrum received by the culture.

When the biomass concentration is low (Fig. 8), in all cases the  $r_{x,\lambda}(r, t)$  profiles follow a pattern quite similar to that of the rate of photon absorption for the same concentration. However, as the cell density of the culture increases (Fig. 9), the values of  $r_{\lambda}^{abs}(r, t)$  increases almost exponentially near the radiation source, while the values of  $r_{x,\lambda}(r, t)$  decrease in these regions, causing a reduction in the biomass production efficiency per photon absorbed. At the same time, the regions of the reactor distant from the LEDs location, present a strong decrease of the biomass production rate, but in this case this is due to the marked decrease of the rate of photon absorption in these regions.

Thus, analyzing the  $r_{x,\lambda}(r, t)$  profiles in Figs. 8 and 9(e)–(h), and the  $r_{\lambda}^{abs}(r, t)$  profiles of the different visible radiation spectrum regions considered Figs. 8 and 9(a)–(d), it is possible to conclude that as cell density increases, the usage of radiation with higher absorption probability (blue and red light) become increasingly inefficient due to a “sieve” effect [34] which causes that these photons be absorbed almost completely within a small distance into the culture, while photons with a low absorption probability (green and yellow light) can travel distances large enough to cause light to be concentrated at the core of the reactor and sustain the cell

growth in areas that can not be reached by the former. Moreover, photons with lower absorption coefficients have higher values of the scattering coefficient [37], so the increment of cell density, will increase the probability of these photons to impact cells and be absorbed (“detour” effect) by increasing the probability of scattering events [34]. These effects would cause that photons with low absorption rates, would be more important in microalgae cultures when high cell densities are reached.

#### 4. Conclusions

In this study the effect of different radiation profiles over microalgal growth was analyzed.

*Scenedesmus quadricauda* respond differently to lighting conditions. Blue radiation profiles promote the increase of chlorophyll concentration in microalgal cells (possibly due to the presence and the activity of a blue light photoreceptor), and a greater biomass production because of the higher absorption coefficients of the blue photons. However, green radiation profiles become more efficient for biomass production in dense microalgal cultures due to the occurrence of “detour” and “sieve” effects.

Kinetic models for growth rate of *Scenedesmus quadricauda* and for the production rate of chlorophylls were proposed. With the proposed kinetic model, it was possible to achieve the correct simulation of different microalgal cultures carried out in two types of PBRs, illuminated with diverse radiation profiles provided by different LEDs arrangements. The results obtained allowed the analysis of the rate of biomass production at each point of the reactor depending on the cell concentration and local radiation properties.

The growth kinetic model obtained along with the radiant field distribution analysis using the physical/mathematical model based on MC method previously developed, proved to be suitable for the simulation of *Scenedesmus quadricauda* cultures under different radiation conditions, being a useful tool for design and optimization of PBRs for the cultivation of microalgae.

#### Acknowledgements

Funds were provided by Universidad Nacional del Litoral, CAI + D 2011 “Análisis, síntesis, simulación y optimización de procesos

biotecnológicos empleando algas microscópicas: cambio de escala racional para la producción de aceites para biodiesel y otras aplicaciones (bio)tecnológicas" and Consejo Nacional de Investigaciones Científicas y Técnicas de la República Argentina (CONICET) PIP 2013 "Procesos biológicos empleando microorganismos fotosintéticos: desarrollo de una plataforma biotecnológica para la producción de biomasa y metabolitos derivados".

## References

- [1] B.F. Cordero, I. Obraztsova, I. Couso, R. León, M.A. Vargas, H. Rodríguez, Enhancement of lutein production in chlorella sorokiniana (Chlorophyta) by improvement of culture conditions and random mutagenesis, *Mar. Drugs* 9 (2011) 1607–1624.
- [2] A. Demirbas, Biodiesel from oilgae, biofixation of carbon dioxide by microalgae: a solution to pollution problems, *Appl. Energy* 88 (2011) 3541–3547.
- [3] Y.C. Jeon, C.W. Cho, Y.S. Yun, Measurement of microalgal photosynthetic activity depending on light intensity and quality, *Biochem. Eng. J.* 27 (2005) 127–131.
- [4] E. Bitaubé Pérez, I. Caro Pina, L. Pérez Rodríguez, Kinetic model for growth of *Phaeodactylum tricornutum* in intensive culture photobioreactor, *Biochem. Eng. J.* 40 (2008) 520–525.
- [5] C.Y. Wang, C.C. Fu, Y.C. Liu, Effects of using light-emitting diodes on the cultivation of *Spirulina platensis*, *Biochem. Eng. J.* 37 (2007) 21–25.
- [6] S.K. Mishra, A. Shrivastava, R.R. Maurya, S.K. Patidar, S. Haldar, S. Mishra, Effect of light quality on the C-phycoerythrin production in marine cyanobacteria *Pseudanabaena* sp. isolated from Gujarat coast India, *Protein Expr. Purif.* 81 (2012) 5–10.
- [7] S. Chandrasekhar, Radiative Transfer, Dover publications Inc., 2000.
- [8] L. Pilon, H. Berberoglu, R. Kandilian, Radiation transfer in photobiological carbon dioxide fixation and fuel production by microalgae, *J. Quant. Spectrosc. Radiat. Transfer* 112 (2011) 2639–2660.
- [9] J.M. Heinrich, I. Niizawa, F.A. Botta, A.R. Trombert, H.A. Irazoqui, Stratification of the radiation field inside a photobioreactor during microalgae growth, *Photochem. Photobiol.* 89 (2013) 1127–1134.
- [10] I. Niizawa, J.M. Heinrich, H.A. Irazoqui, Modeling of the influence of light quality on the growth of microalgae in a laboratory scale photo-bio-reactor irradiated by arrangements of blue and red LEDs, *Biochem. Eng. J.* 90 (2014) 214–223.
- [11] J. Pruvost, J. Legrand, P. Legentilhomme, A. Muller-Feuga, Simulation of microalgae growth in limiting light conditions: flow effect, *AIChE J.* 48 (2002) 1109–1120.
- [12] J.F. Cornet, C.G. Dussap, J.B. Gross, C. Binois, C. Lasseur, A simplified monodimensional approach for modeling coupling between radiant light transfer and growth kinetics in photobioreactors, *Chem. Eng. Sci.* 50 (1995) 1489–1500.
- [13] Q. Huang, T. Liu, J. Yang, L. Yao, L. Gao, Evaluation of radiative transfer using the finite volume method in cylindrical photoreactors, *Chem. Eng. Sci.* 66 (2011) 3930–3940.
- [14] J. Dauchet, S. Blanco, J. Cornet, M.E. Hafi, V. Eymet, R. Fournier, The practice of recent radiative transfer Monte Carlo advances and its contribution to the field of microorganisms cultivation in photobioreactors, *J. Quant. Spectrosc. Radiat. Transfer* 128 (2013) 52–59.
- [15] Y. Zhao, J. Wang, H. Zhang, C. Yan, Y. Zhang, Effects of various LED light wavelengths and intensities on microalgae-based simultaneous biogas upgrading and digestate nutrient reduction process, *Bioresour. Technol.* 136 (2013) 461–468.
- [16] Z.H. Kim, H.S. Lee, C.G. Lee, Red and blue photons can enhance the production of astaxanthin from *haematococcus pluvialis*, *Algae* 24 (2009) 121–127.
- [17] H. Jeong, J. Lee, M. Cha, Energy efficient growth control of microalgae using photobiological methods, *Renew. Energ.* 54 (2013) 161–165.
- [18] S.H. Lee, J.E. Lee, Y. Kim, S.Y. Lee, The Production of High Purity Phycocyanin by *Spirulina platensis* Using Light-Emitting Diodes Based Two-Stage Cultivation, *178* (2016) 382–395.
- [19] W. Fu, O. Gudmundsson, A.M. Feist, G. Herjolfsson, S. Brynjolfsson, B.O. Palsson, Maximizing biomass productivity and cell density of *Chlorella vulgaris* by using light- emitting diode-based photobioreactor, *J. Biotechnol.* 161 (2012) 242–249.
- [20] C.Y. Wang, C.C. Fu, Y.C. Liu, Effects of using light-emitting diodes on the cultivation of *Spirulina platensis*, *Biochem. Eng. J.* 37 (2007) 21–25.
- [21] M. Atta, A. Idris, A. Bukhari, S. Wahidin, Intensity of blue LED light: a potential stimulus for biomass and lipid content in fresh water microalgae *Chlorella vulgaris*, *Bioresour. Technol.* 148 (2013) 373–378.
- [22] W. Fu, Ó. Guðmundsson, G. Paglia, G. Herjólfsson, Ó.S. Andrésson, B.O. Palsson, S. Brynjólfsson, Enhancement of carotenoid biosynthesis in the green microalga *Dunaliella salina* with light-emitting diodes and adaptive laboratory evolution, *Appl. Microbiol. Biotechnol.* 97 (2013) 2395–2403.
- [23] V.B. Borodin, Effect of red and blue light on acclimation of *Chlamydomonas reinhardtii* to CO<sub>2</sub>-limiting conditions, *Russ. J. Plant Physiol.* 55 (2008) 441–448.
- [24] H. Takano, T. Arai, M. Hirano, T. Matsunaga, Effects of intensity and quality of light on phycocyanin production by a marine cyanobacterium *Synechococcus* sp. NKBG 042902 H, *Appl. Microbiol. Biotechnol.* 43 (1995) 1014–1018.
- [25] Y.C. Jeon, C.W. Cho, Y.S. Yun, Measurement of microalgal photosynthetic activity depending on light intensity and quality, *Biochem. Eng. J.* 27 (2005) 127–131.
- [26] D. Hermsmeier, E. Eleni Mala, R. Schulz, J. Thielmann, P. Galland, H. Senger, Antagonistic blue and red-light regulation of cab-gene expression during photosynthetic adaptation in *Scenedesmus obliquus*, *J. Photochem. Photobiol. B* 11 (1991) 189–202.
- [27] S. Masuda, Light detection and signal transduction in the BLUF photoreceptors, *Plant Cell Physiology* 54 (2013) 171–179.
- [28] N. Yeh, J.P. Chung, High-brightness LEDs—Energy efficient lighting sources and their potential in indoor plant cultivation, *Renew. Sustain. Energy Rev.* 13 (2009) 2175–2180.
- [29] Z. Tukaj, The effects of crude and fuel oils on the growth, chlorophyll 'a' content and dry matter production of a green alga *Scenedesmus quadricauda* (Turp.) bréb, *Environ. Pollut.* 47 (1987) 9–24.
- [30] R.J. Ritchie, Consistent sets of spectrophotometric chlorophyll equations for acetone, methanol and ethanol solvents, *Photosynth. Res.* 89 (2006) 27–41.
- [31] S. Aiba, Growth kinetics of photosynthetic microorganisms, *Adv. Biochem. Eng.* 23 (1982) 85–156.
- [32] J. Masojídek, M. Kobližek, G. Torzillo, Photosynthesis in microalgae, in: A. Richmond (Ed.), *Handbook of Microalgal Culture: Biotechnology and Applied Phycology*, Blackwell Science, UK, 2016, pp. 20–40.
- [33] M.C.A.F. Rezende, C.B.B. Costa, A.C. Costa, M.R. Wolf Maciel, R. Maciel Filho, Optimization of a large scale industrial reactor by genetic algorithms, *Chem. Eng. Sci.* 63 (2008) 330–341.
- [34] I. Terashima, T. Fujita, T. Inoue, W.S. Chow, R. Oguchi, Green light drives leaf photosynthesis more efficiently than red light in strong white light: revisiting the enigmatic question of why leaves are green, *Plant Cell Physiol.* 50 (2009) 684–697.
- [35] K. Humbeck, B. Hoffmann, H. Senger, Influence of energy flux and quality of light on the molecular organization of the photosynthetic apparatus in *Scenedesmus*, *Planta* 173 (1998) 205–212.
- [36] A. Moglich, X. Yang, R.A. Ayers, K. Moffat, Structure and function of plant photoreceptors, *Annu. Rev. Plant Biol.* 61 (2010) 21–47.
- [37] J.M. Heinrich, I. Niizawa, F.A. Botta, A.R. Trombert, H.A. Irazoqui, Analysis and design of photobioreactors for microalgae production I: Method and parameters for radiation field simulation, *Photochem. Photobiol.* 88 (2012) 938–9510.